NUMERICAL METHODS TO GENERATE SOLAR SAIL TRAJECTORIES

Kathleen Howell
Purdue University

NUMERICAL METHODS TO GENERATE SOLAR SAIL TRAJECTORIES

Geoffrey G. Wawrzyniak and Kathleen C. Howell
Purdue University, West Lafayette, Indiana
gwawrzyn@purdue.edu

ABSTRACT

Solar sail trajectory design often requires a transition from analytical models to numerically generated realizations of an orbit. As one type of numerical scheme, differential correctors, also known as shooting methods, are commonly used in astrodynamics. Finite-difference methods and collocation schemes are also employed and are successful in generating trajectories with continuous control histories. All methods reveal parts of the design space for solar sail applications.

INTRODUCTION

Generating spacecraft trajectories in multi-body regimes to meet mission requirements is not easy. Generating *solar sail* trajectories in multi-body regimes is even more challenging. Trajectory design for any spacecraft mission application typically involves either well-developed analytical approximations or a linearization relative to a known solution. These approximations are typically based on well-understood dynamics. However, when two or more large bodies (e.g., Earth and Moon, or Sun, Earth, and Moon) are present, trajectories in a multi-body gravitational field can become chaotic. The problem is further complicated when an additional force from a solar sail is incorporated.

Various authors have recently demonstrated that a solar sail spacecraft can potentially support a communications architecture for an outpost at the lunar south pole (LSP) [1–4]. These analyses are usually formulated within an Earth–Moon circular restricted three-body (EM-CR3B) model. However, this frame poses new challenges for solar sail mission design because the Sun moves with respect to a fixed Earth and Moon; analytical tools may not always reveal desired, or even viable, solutions.

Certainly, analytical perturbation approaches are available for solar sail trajectory design in two- and three-body regimes, and in frames where the Sun is stationary or is moving. However, recent work using numerical techniques for solving boundary value problems (BVPs) shows promise for uncovering solutions to problems of spacecraft trajectory design involving solar sails [1–3]. Numerical strategies for solving BVPs, such as shooting (or differential-corrections processes), finite-difference methods, as well as collocation, greatly expands the range of the available design space for trajectories in severely nonlinear or chaotic dynamical systems. Numerical methods may require little knowledge of the complicated dynamical structure to initiate the process. Furthermore, new mission opportunities, options not deduced via analytical techniques, may emerge.

A brief description of the behavior of solar sail spacecraft in the EM system is first introduced. An overview of the differential corrections processes for solar sail trajectories is followed by a discussion of finite-difference methods, then collocation. Other numerical tools for generating orbits do exist, but are left for future investigations. While these numerical methods may be used as part of an optimization scheme, optimization is not discussed here. Finally, some examples using the solution from one technique to initialize a different strategy are summarized.

1 DYNAMICAL MODEL

The vector equations of motion, formulated in terms of coordinates rotating relative an inertial frame, for a spacecraft in a CR3B system and located approximately one AU from the Sun, are

$$\ddot{\mathbf{r}} + 2\boldsymbol{\omega} \times \dot{\mathbf{r}} + \boldsymbol{\nabla} U - \frac{a_0}{a^*}(\hat{\boldsymbol{\ell}}(t) \cdot \mathbf{u})^2 \mathbf{u} = 0 \tag{1}$$

where $\boldsymbol{\nabla} U$ is the gradient of a pseudo-potential that includes the centripetal and the gravity effects of the two primaries. Vectors are denoted in boldface. The final term in Eq. (1) represents the acceleration of the sail, non-dimensionalized by the system acceleration, a^* (2.73 mm/s^2 for the EM system); a_0 is the sail's characteristic acceleration at one AU, $\hat{\boldsymbol{\ell}}(t)$ is the sunlight direction, and $\mathbf{u}$ is the direction of the sailface normal. The angle between the sail normal and the sun-line is commonly denoted α, and equals $\cos^{-1}(\hat{\boldsymbol{\ell}}(t) \cdot \mathbf{u})$. The Sun moves about the EM system at a rate of Ω, that is, the ratio of the synodic rate to the sidereal rate (approximately 0.925), and, thus, $\hat{\boldsymbol{\ell}}(t) = \left\{ \begin{array}{ccc} \cos \Omega t & -\sin \Omega t & 0 \end{array} \right\}$. The EM-system model is illustrated in Fig. 1. The Sun is assumed to be infinitely far from the system such that solar gravity is negligible and the rays of sunlight are parallel.

Since the acceleration from the sail is time variant, equilibria in the EM system exist only when $\alpha = 90°$ or $a_0 = 0$; the five classical Lagrange points are then the equilibrium points. In applications where the Sun and the Earth are the primaries (e.g., SE-CR3B model, where $a^* = 5.93$ mm/s^2), $\hat{\boldsymbol{\ell}}$ is stationary within the reference frame and parallel to the Sun–sail vector. Surfaces of stationary points, or equilibrium surfaces, exist in the SE-CR3B system and supply a large solution space from which orbits may be developed using analytical techniques. In the EM system, only instantaneous surfaces can be computed. Nevertheless, periodic orbits do exist in the EM system and are examined.

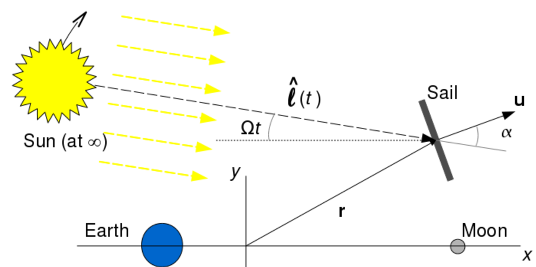

Fig. 1: EM system model.

2 DIFFERENTIAL CORRECTORS (SHOOTING)

Shooting methods, often termed differential corrections (DC) processes, are common tools for generating trajectories in astrodynamics. In general, some sort of approximation is developed via analytical methods that incorporate knowledge of the system dynamics. Often, a trajectory is approximated via a linearization relative to a known reference solution to the nonlinear differential equations, such as an equilibrium point. States from this approximation are used to initialize numerical integration of the nonlinear equations of motion. A state transition matrix (STM) is propagated along with a six-state (position and velocity) trajectory and is used to linearly correct the states and, thus, select the initial values of the elements. Dynamical characteristics extracted from the STM are very effective and, as a result, DC is a popular tool for generating orbits. Multiple shooting [5] and two-level correctors [6] exploit short arc segments, usually along non-periodic orbits, for a more stable numerical solution; path constraints (e.g., elevation) and continuity between arc segments are enforced at the endpoints along each segment. The sail attitude is generally fixed along each arc segment (or the whole orbit if single shooting is employed).

Nuss [7] and A. McInnes [8] both use shooting methods to generate halo orbits in the SE-CR3B regime. Nuss begins with a third-order approximation for a halo orbit about a collinear Lagrange point (L_1), used shooting to deliver a nonlinear solution, and then applies continuation based on a_0 to extend the nonlinear, solar sail halo orbits toward the Sun [7]. A. McInnes expands the approximation to include solar sail effects and generates families about artificial Lagrange points for various a_0 [8]. In Waters and C. McInnes [9], a DC process is employed to correct Lindstedt-Poincaré approximations of periodic orbits above the SE ecliptic plane. Likewise, Farrés and Jorba [10] employ multiple shooting as a tool to compute periodic orbits near the Sun–Earth–Sail L_1 point.

As an example of the computation of a solar sail trajectory using shooting in the EM problem, a linear approximation for elliptical orbits below the Lagrange points and parallel to the EM orbit plane is detailed in Simo and McInnes [4]. In these orbits, the pitch angle, α, is fixed to supply a constant out-of-plane force; based on the linearized equations of motion, the pitch angle that supplies the maximum out-of-plane force is $35.264°$. The orbits in [4] are plotted directly from the approximation. To compute periodic nonlinear orbits, the Simo-McInnes approximation is used to seed a DC scheme here. The process is developed to determine a family of periodic orbits in the nonlinear model. The initial state, as specified on the xz plane, from a linear approximation corresponding to an out-of-plane orbit in [4] supplies an initial guess for a nonlinear trajectory that is corrected by the DC scheme. An STM is constructed based on the variations of $\mathbf{r}$, $\dot{\mathbf{r}}$, and a_0 such that deviations at the beginning of the arc, $\{\delta\mathbf{r}_i \ \delta\dot{\mathbf{r}}_i \ \delta(a_0)\}$, are linearly mapped to some future time, $\{\delta\mathbf{r}_f \ \delta\dot{\mathbf{r}}_f\}$. A deviation in $\mathbf{r}$ is computed as $\delta\mathbf{r} = \mathbf{r}_d - \mathbf{r}_a$, where $\mathbf{r}_d$ is the desired value of $\mathbf{r}$ and $\mathbf{r}_a$ is the actual value. Given the characteristics of this dynamical system, a periodic orbit is assumed to be symmetric across the xz plane, thus, (1) the plane crossings are perpendicular, (2) t_f can be set to the half-period, or the second crossing of the xz plane, and (3) a reduced set of variables is required for the DC process. These propositions suggest that $\{\delta y_f \ \delta\dot{x}_f \ \delta\dot{z}_f\}$ can deliver either $\{\delta x_i \ \delta\dot{y}_i \ \delta(a_0)\}$ or $\{\delta z_i \ \delta\dot{y}_i \ \delta(a_0)\}$, depending on the advantages in fixing z_i or x_i, respectively, over a set of iterations for a particular orbit. An updated state, $\{\mathbf{r}_i \ \dot{\mathbf{r}}_i \ a_0\}$, is then used to re-initialize the trajectory. Characteristic acceleration, a_0, remains constant along the orbit. The process is repeated until a convergence tolerance is met. A family of orbits that is initialized by the linear approximation in [4] appears in Fig. 2. The color associated with each orbit in the figure represents the characteristic acceleration, a_0, that is required to produce the corresponding path. The approximation from [4] to initialize the DC process is successful in producing periodic orbits for out-of-plane distances from zero to about 300 km below the EM orbit plane (an ellipse 100 km in x and 1900 km in y). Thereafter, a continuation scheme is employed, using the initial states from the previous orbits to predict the initial state for the current orbit. It is notable that the black orbit in Fig. 2 coincides with a bifurcation in the eigen-structure, indicating a branching to another family of orbits. Shortly after this first bifurcation, the continuation procedure along the family yields the orbits that require a maximum characteristic acceleration level equal to 1.6 mm/s^2. Other bifurcations along this family are also observed, indicating intersections with other families of solutions. The family of nonlinear orbits represented in Fig. 2 clearly does not produce trajectories with continuous communications coverage at the LSP, but demonstrates the DC process.

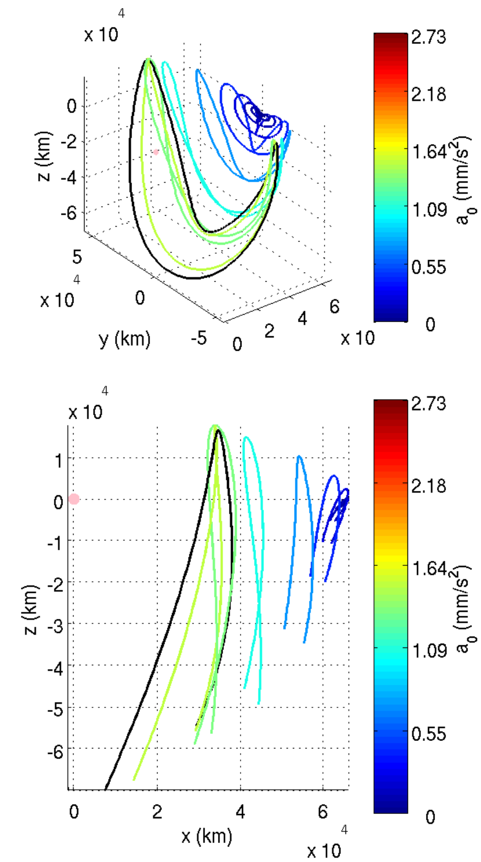

Fig. 2: A family of offset orbits in the vicinity of L_2. The Moon is pink and is plotted for scale.

The accuracy of a shooting method depends on the iteration and integration tolerances, as well as the model itself. The deviations at the end of a propagation sequence are compared to iteration tolerances to determine convergence. The preceding example employed MATLAB®'s ODE113 explicit integration routine to propagate the orbits [11]. Similar to other MATLAB® propagators, the theoretical error associated with each propagated state at a step is compared to relative and absolute integration tolerances to control step size. In theory, a propagated trajectory could diverge from a true trajectory, but the likelihood is reduced with tighter tolerances. Consequently, propagated trajectories are often regarded as "truth" models in mission design.

3 FINITE-DIFFERENCE METHODS

Rather than computing variations relative to a reference solution, finite-difference methods (FDMs) approach the trajectory "as a whole" [3]. A very simple guess, such as a circle or a point, is discretized into $\{\mathbf{r}_1, \ldots, \mathbf{r}_i, \ldots, \mathbf{r}_n\}$ at n node points along the trajectory. Vector derivatives of the state vector are approximated by central differences. These approximations substitute for the true time derivatives in Eq. (1). If the initial guess for the path does not satisfy the equations of motion (usually the case), Eq. (1) is not equal to the value of the approximation. Other constraints, such as periodicity, magnitude of the unitary control direction ($\|\mathbf{u}_i\| = 1$), path constraints (elevation, altitude, etc.), are formulated as equality constraints and are functions of the discretized path coordinates (all $\mathbf{r}_i$), control vector (all $\mathbf{u}_i$), and slack variables (all $\boldsymbol{\eta}_i$, which convert inequality path constraints into equality constraints) at each node. A Newton-Raphson iteration scheme is used to solve for the set of $\mathbf{r}_i$, $\mathbf{u}_i$, and $\boldsymbol{\eta}_i$ that satisfy the Eq. (1).

The advantage of FDMs is their simplicity in terms of understanding and implementation, especially with time-dependent control profiles. The disadvantage is that the local accuracy is limited to $\mathscr{O}(\Delta t^2)$ as $\Delta t \to 0$, or the number of nodes, n, grows. The number of equations to be solved and the integration round-off error increase as n gets larger. Sample FDM solutions appear in Fig. 3. These orbits are generated with a minimum elevation constraint of 15° as viewed from the LSP. The Moon is pink and to scale, and $L_{1,2}$ appear as black dots. Trajectories integrated with MATLAB®'s ODE113 [11], those that are initialized with states and control histories from the FDM solutions, also appear in Fig. 3. From an initial state near L_2, each integrated solution follows the path and velocity associated with the FDM solution for part of the orbit, but diverges, in part, because of dynamical and numerical sensitivities, as well as the fact that the control history, $\mathbf{u}(t)$, and initial state do not satisfy Eq. 1 exactly. Note that the integrated trajectory using states from the blue orbit diverges from the original path and loops around the Moon. It may be possible, however, that the trajectory approximated with a FDM can be used to initialize a more accurate numerical technique. Another possibility is that an FDM solution is sufficiently accurate such that small adjustments to the states and control can produce a more accurate solution or small adjustments solely to the control will allow tracking of a specified solution as a reference. In any case, the design space for this problem is not well known, so a trajectory that solves the equations of motion to within a small error is meaningful. If the goal is a general understanding of the design space, accomplished in a relatively quick analysis, then results from a FDM approximation can stand alone and be very insightful.

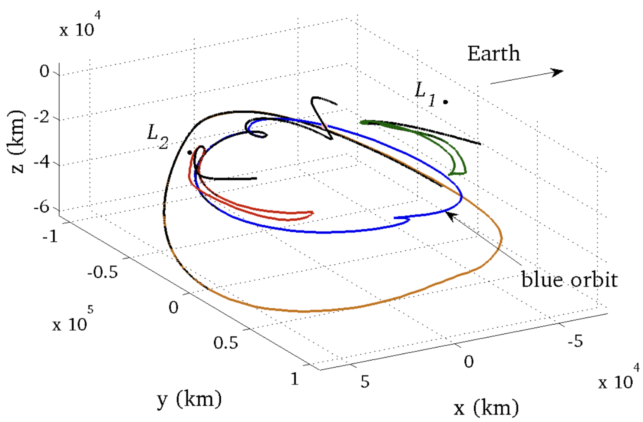

Fig. 3: FDM orbits. Half-period propagations of initial states from FDM orbits are in black.

4 COLLOCATION

Similar to FDMs, a collocation scheme also discretizes the trajectory and control, and then delivers a solution for the discretized control and trajectory states simultaneously. Collocation involves minimization of the difference between the derivative of a continuous approximating polynomial and the derivative from the equations of motion at an intermediate, or defect, point (or points) on an arc between nodes along a trajectory. While the accuracy of FDMs is limited to the step size between nodes, collocation offers more accuracy by selecting higher-degree polynomials.

Because of their relative insensitivity to a poor initial guess and relative accuracy when compared to other approaches, collocation methods are increasingly common for solving BVPs, including optimal control problems. Optimization software packages such as DIDO and GPOPS, as well as MATLAB®'s BVP*C functions (* = 4,5,6), rely on collocation. The type of polynomial and integration rules vary for different accuracies. Nassiri et al. [12] employ a technique that relies on a Hermite interpolating polynomial and Simpson quadrature rules (a.k.a., Hermite-Simpson collocation), which possess a local accuracy of $\mathscr{O}(\Delta t^5)$, to minimize the time of flight along a solar sail interplanetary transfer. Ozimek et al. [1] demonstrate (1) a Hermite-Simpson collocation scheme for a solar sail in the EM system, and (2) a highly accurate scheme for the same system that is based on a seventh-degree polynomial subject to Gauss-Lobatto integration constraints with a local accuracy of $\mathscr{O}(\Delta t^{12})$; both employ equally spaced nodes.

In Ozimek et al. [2], mesh refinement is employed in the seventh-degree Gauss-Lobatto scheme, strategically redistributing and reducing the number of nodes required for a solution of equal accuracy across all nodes. The initial guess from which these orbits are produced is a trajectory that is a stationary point in the EM rotating frame with a sail pitch angle of $\alpha = 35.264°$; the resulting orbits are periodic and have time-varying control profiles. Ozimek et al. provide conditions for explicit integration for the five orbits originally uncovered by this scheme [2]. Results using these conditions to numerically propagate orbits for one period appear in Fig. 4. As stated by the authors in [2], the blue and green orbits possess a minimum elevation of 4.2° and 6.8°, respectively. The other three orbits (red, magenta, and gray) all meet a minimum elevation constraint of 15°. Similar to FDMs, collocation returns the required control history, $\mathbf{u}(t)$, as well as states along the trajectory. Unlike the FDM, a propagation based on these states and the specified control history often results in a solution that resembles the Gauss-Lobatto collocation solution. However, this observation in no way implies that solutions from one numerical approach are superior to those emerging from another method. Each periodic orbit generated here can serve as a reference trajectory for mission design. Naturally, navigation and flight-path control must be considered for an actual flight as model uncertainties and mismodeling result in an actual trajectory that diverges from the reference.

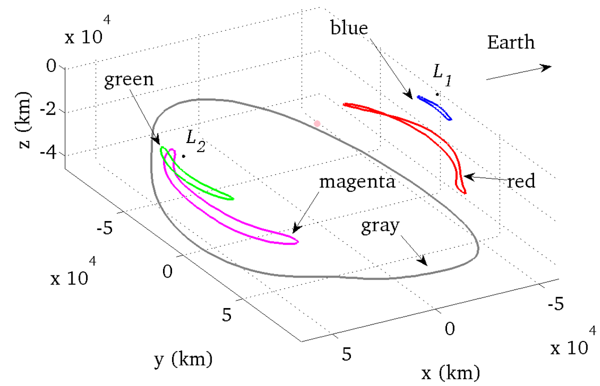

Fig. 4: Propagated orbits from Ozimek et al. [2].

5 BOOTSTRAPPING DIFFERENT NUMERICAL METHODS

Solutions that result from the application of the various methods possess theoretical local accuracies of $\mathscr{O}(\Delta t^n)$, where n is some integer, that is, the evaluation of the left side of Eq. (1) produces a value that is within $\mathscr{O}(\Delta t^n)$ of zero at a give node. This small difference does not necessarily imply that the numerical solution is close to an unknown true solution. Therefore, it cannot be assumed that a solution from a lower-accuracy method will always successfully initialize a higher-accuracy method. However, lower-accuracy solutions frequently add insight and sometimes offer valuable initial guess options for other methods in a process known as "bootstrapping."

The orbits generated by the FDM *nearly* solve Eq. (1). However, as demonstrated in Fig. 3 and due to a number of contributing factors, the explicit integration of position and velocity states from an FDM solution, along with a complete control history from the FDM analysis, diverges from the reference orbit. Mission designers are left with various options. One possibility is to control to the reference path, either by incorporating a second form of control [4] or via small adjustments to the control profile; either control technique may yield an infeasible trajectory without additional processing. Alternatively, the reference trajectory might also be pre-processed, that is, refined in advance using a more accurate numerical method.

One approach to refine a trajectory from an FDM solution is to use collocation. The blue orbit (position, velocity, and control history) from Fig. 3 is used to initialize a Hermite-Simpson collocation scheme, resulting in the cyan orbit that appears in Fig. 5. A trajectory is numerically integrated using the updated control history and initialized with a state from the cyan orbit. The resulting path is represented in black in Fig. 5. This propagated trajectory overlays the cyan reference orbit for more than a quarter orbit,

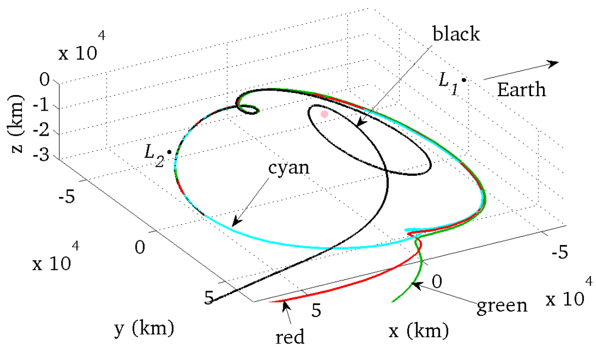

Fig. 5: Trajectories generated by bootstrapping an FDM orbit.

indicating that the collocation-updated trajectory yields more precise position and velocity states as well as control history. Alternatively, a single-shooting approach is employed to correct the initial state from the blue FDM orbit in Fig. 3. The green path in Fig. 5 is generated by enforcing a perpendicular crossing of the xz plane at a fixed time corresponding to one half of the specified period of the orbit; the velocity in the y direction at the beginning of the orbit is corrected to produce periodicity. Finally, the cyan orbit generated by the collocation update is similarly corrected with a single shooting, resulting in the red path in Fig. 5. All integrations are for a full period. Both the green and red trajectories perform as expected for the first half-period. However, they are not perfectly periodic and diverge after the first half-period. At least three possibilities exist for the lack of periodicity: (1) the solution is dynamically and numerically sensitive, (2) a true solution does not exist near the cyan reference path, or (3) the control history, which is *not* differentially corrected with the states, does not accurately solve the EOMs. While not investigated here, with additional complexity in the algorithm, shooting might also be used to correct the control history. Nevertheless, the red and green paths represent a significant improvement to the performance of the cyan approximation.

CONCLUSIONS

The numerical methods described here are useful tools for uncovering solar sail trajectories in complex dynamical regimes. These methods complement analytical approaches and approximations. Lower-accuracy results may sometimes initialize higher-accuracy solutions. Additionally, since the numerical solutions nearly solve the equations of motion, some form of adjustment to the control might be employed to complete a periodic solution or meet other trajectory goals; future efforts will address this issue.

ACKNOWLEDGEMENTS

The authors would like to thank Martin Ozimek and Daniel Grebow for their insights. The first author thanks the Purdue Graduate Student Government and NASA Academy's Dr. Gerald A. Soffen Memorial Fund for the Advancement of Space Science Education for their sponsorship through travel grants.

REFERENCES

[1] M. T. Ozimek, D. J. Grebow, and K. C. Howell, *Journal of Guidance, Control, and Dynamics* **32**, 1884 (2009).
[2] M. T. Ozimek, D. J. Grebow, and K. C. Howell, A Collocation Approach for Computing Solar Sail Lunar Pole-Sitter Orbits, in *AAS/AIAA Astrodynamics Specialists Conference*, Pittsburgh, Pennsylvania, 2009, Paper AAS 09-378.
[3] G. G. Wawrzyniak and K. C. Howell, Accessing the Design Space for Solar Sails in the Earth–Moon System, in *AAS/AIAA Astrodynamics Specialists Conference*, Pittsburgh, Pennsylvania, 2009, Paper AAS 09-348.
[4] J. Simo and C. McInnes, *Journal of Guidance, Control, and Dynamics* **33**, 259 (2010).
[5] J. Stoer and R. Bulirsch, *Introduction to Numerical Analysis*, Springer-Verlag, New York, 3rd edition, 2002.
[6] K. C. Howell and H. J. Pernicka, *Celestial Mechanics* **41**, 107 (1988).
[7] J. S. Nuss, *The Use of Solar Sails in the Circular Restricted Problem of Three Bodies*, Masters Thesis, Purdue University, West Lafayette, Indiana, 1998.
[8] A. I. S. McInnes, *Strategies for Solar Sail Mission Design in the Circular Restricted Three-Body Problem*, Masters Thesis, Purdue University, West Lafayette, Indiana, 2000.
[9] T. J. Waters and C. R. McInnes, *Journal of Guidance, Control, and Dynamics* **30**, 687 (2007).
[10] A. Farrés and Àngel Jorba, *Celestial Mechanics and Dynamical Astronomy* (2010), DOI: 10.1007/s10569-010-9268-4.
[11] The MathWorks™, Inc., *MATLAB®, Version 7.9.0 (R2009b)*, Natick, Massachusetts, 2009, *www.mathworks.com*.
[12] N. Nassiri, N. Mehdizadeh, and M. Jalali, Interplanetary flight using solar sails, in *RAST 2005. 2nd International Conference on Recent Advances in Space Technologies*, pp. 330–334, Istanbul, Turkey, 2005.